Transverse Migration of a Confined Polymer Driven by an External Force

O. Berk Usta, Jason E. Butler, and Anthony J. C. Ladd*

Department of Chemical Engineering, University of Florida, Gainesville, Florida 32611, USA
(Received 10 November 2006; published 26 February 2007)

We demonstrate that a polymer confined to a narrow channel migrates towards the center when driven by an external force parallel to the channel walls. This migration results from asymmetric hydrodynamic interactions between polymer segments and the confining walls. A weak pressure-driven flow, applied in the same direction as the external force, enhances the migration. However, when the pressure gradient and the external force act in opposite directions the polymer can migrate towards the boundaries. Nevertheless, for sufficiently strong forces the polymer always migrates towards the center. A dumbbell kinetic theory explains these results qualitatively. A comparison of our results with experimental measurements on DNA suggests that hydrodynamic interactions in polyelectrolytes are only partially screened. We propose new experiments and analysis to investigate the extent of the screening in polyelectrolyte solutions.

PACS numbers: 47.57.Ng, 47.15.G−, 47.27.nd

Flexible polymers in a pressure-driven flow field migrate towards the center of the channel, because of hydrodynamic interactions. The local shear rate stretches the polymer and the resulting tension in the chain generates an additional flow field around the polymer. This flow field becomes asymmetric near a no-slip boundary and results in a net drift towards the center of the channel [1–3]. Recent simulations [3,4] show that hydrodynamic lift is the dominant migration mechanism in pressure-driven flow, rather than spatial gradients in shear rate. Since the migration depends on chain length [2,4], it is in principle possible to fractionate polymers based on their length; longer polymers migrate more strongly and therefore elute faster. However, Taylor dispersion precludes any sharply peaked distribution, and so there is considerable interest in using combinations of flow and electric fields to improve separation efficiency [5]. We used numerical simulations to investigate a flexible polymer driven by a combination of fluid flow and external force. In this preliminary investigation we have not considered the effects of counterion screening. We find that the polymer migrates towards the channel center under the action of a body force alone, while in combination with a pressure-driven flow, the polymer can move either towards the channel wall or towards the channel center. A kinetic theory, based on a dumbbell model of the polymer, gives a qualitative understanding of the results. The simulations mimic recent experimental observations of the migration of DNA in combined electric and pressure-driven flow fields [6,7]. The similarities between these results suggest that hydrodynamic interactions in polyelectrolyte solutions are only partially screened [8].

Numerical simulations were used to investigate the motion of a confined polymer chain driven by a combination of fluid flow and external forces. The system is bounded in one direction by no-slip walls with a separation $H \sim 8$–$16 R_g$, where R_g is the equilibrium radius of gyration. Periodic boundaries were used in the other two directions,

with a repeat length ($L = 2H$) such that the hydrodynamic interactions between periodic images are negligible [9]. The external field and pressure gradient result in two different Peclet numbers: $\mathrm{Pe} = \bar{U} R_g / D$ and $\mathrm{Pe}_f = \bar{\gamma} R_g^2 / D$. Here $\bar{U}$ is the average polymer velocity with respect to the fluid, D is the free-solution diffusion coefficient, and $\bar{\gamma}$ is the average shear rate. We employ a hybrid algorithm, coupling point particles connected by stiff springs to a Newtonian fluid [10]. The fluid is simulated by a fluctuating lattice-Boltzmann equation [11], which accounts quantitatively for the dissipative and fluctuating hydrodynamic interactions between polymer segments [9]. The polymer chains were discretized into $N - 1$ segments of length $b = \Delta$, where Δ is the lattice spacing. Most simulations used $N = 16$, with a radius of gyration $R_g \approx 2\Delta$, but additional simulations with $N = 32$ were used to ensure that the effect of chain discretization on the polymer distribution was small. A detailed description of the numerical method can be found in Ref. [9].

The numerical simulations show that a flexible polymer chain migrates towards the channel center when subjected to a strong external force parallel to the channel boundaries. At Peclet numbers in excess of 100, this transverse migration results in a nonuniform center of mass distribution (Fig. 1), with the polymer concentrated in the middle of the channel. For small forces ($\mathrm{Pe} < 10$), Brownian motion is dominant and the distribution eventually becomes uniform, except for a small depletion layer near the channel walls. However, if hydrodynamic interactions are neglected there is no migration, and the distribution is uniform at all Peclet numbers. This observation emphasizes the hydrodynamic origin of the migration.

In the limit of infinite Peclet number the distribution still has a finite width, which shows that flexible polymers have an additional dispersive mechanism besides Brownian motion. Each segment, driven by the external force, sets up a long-range flow field, which perturbs the velocity of surrounding segments. The velocity of each segment then
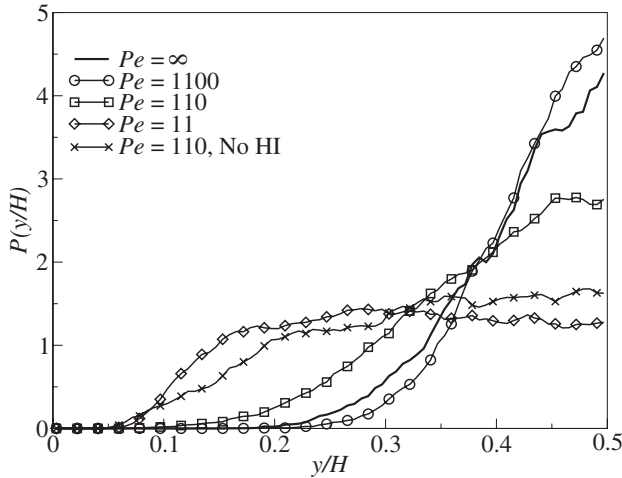
FIG. 1.   Center of mass distribution of a single polymer in a channel $H/R_g = 8$ under the application of an external body force. Half of the distribution is shown, with the boundary at $y/H = 0$ and the center of the channel at $y/H = 0.5$.

fluctuates in time with changing segment positions, leading to diffusion of the polymer center of mass and relaxation of polymer conformations towards the coiled state. This is similar to the hydrodynamic dispersion in settling suspensions [12], and plays an important role in limiting the migration at high Peclet numbers. A polymer in the vicinity of a wall rotates due to hydrodynamic interactions with the boundary and drifts away from the wall. However, the drifting polymer changes conformation through hydrodynamic dispersion, eventually assuming a more spherical shape which limits further drift. Without this dispersion the polymer would traverse back and forth across the channel, similar to a rigid rod [13], and the time-averaged center of mass distribution across the channel would then be uniform. However, a flexible polymer achieves a nonuniform distribution at high Peclet numbers because its drift velocity diminishes as it gets further from the wall and assumes a more spherical shape. On the other hand a rigid spherical particle would not migrate at all and the distribution would again be uniform, due to the small residual Brownian motion. Flexibility and hydrodynamic dispersion are therefore crucial in determining the distribution at large Peclet numbers. The hydrodynamic dispersion can be as large as Brownian diffusion, as can be seen by comparing the width of the infinite Peclet distribution, where there is no Brownian motion, with a finite Peclet number case, Pe = 1100 (see Fig. 1). Note that the statistical errors for the infinite Peclet case are approximately 10%, so these distributions are statistically indistinguishable. Thus hydrodynamic dispersion dominates Brownian diffusion by a Peclet number of 1000.

A theoretical approach can be used to gain further insight into the hydrodynamic origin of the migration. We used a kinetic theory similar to Ref. [3] and have identified three mechanisms that lead to migration: two have been

noted previously [3,6]; one is new. We analyzed the evolution of the distribution function of a dumbbell near a planar boundary, incorporating a uniform external field in addition to the linear shear flow [3]. The key assumption is that the distribution function can be factored into a product of the center of mass distribution, $P(y, t)$, and the orientation distribution, where y is the distance of the center of mass from the boundary. We have further assumed that the dumbbell is connected by a linear spring and that the orientation distribution can be expanded in powers of the local shear rate and external force. The calculation will be described more fully in a subsequent paper, which will include a quantitative comparison between theory and simulation. Here we simply note the final result for the steady-state center of mass distribution function, $P(y)$, near a planar boundary,

$$\frac{\partial}{\partial y^*}\left[Aa^* \frac{\mathrm{Pe}_f^2}{y^{*2}} + Ba^{*2}\frac{\mathrm{Pe}^2}{y^{*2}} \pm Ca^*\mathrm{Pe}_f\mathrm{Pe} - \frac{\partial}{\partial y^*}\right]P = 0. \tag{1}$$

The distance from the wall $y^* = y/R_g$ and hydrodynamic radius $a^* = a/R_g$ have been scaled by R_g; in the numerical simulations $a^* = 0.125$. The sign of the mixed term depends on whether the force and flow are applied in conjunction $(+)$ or opposition $(-)$. A, B, and C are numerical coefficients: $A = 1/32$, $B = 9/160\sqrt{6\pi}$, and $C = 1/20\sqrt{6\pi}$. As in Ref. [3], the solution for a dumbbell near a single wall can be extended to a channel flow by superposing the solutions for the two walls and using a spatially varying shear rate.

The first term in Eq. (1) describes the lift created for the center of mass of a dumbbell by the asymmetric hydrodynamic interactions between the polymer segments and the walls [3]. The local shear rate generates a tension in the polymer, which creates a nonuniform distribution in pressure-driven flows as seen in recent experiments [1] and simulations [2,4,9]. The second term describes the rotation and drift of the polymer towards the channel center under the application of an external field. Although both terms arise from hydrodynamic interactions with a boundary, the mechanisms are different in the motion they create. In a shearing flow the polymer is in tension, and the opposing forces generate a lift for the center of mass [3] [see Fig. 2(a)], but in an external field the force on the monomers has the same sign, which causes the polymer to rotate away from the boundary [see Fig. 2(b)]. Subsequently, the polymer drifts towards the center under the action of the force. Finally, there is a cross term that arises from a coupling between the stretching and rotation of the polymer by the flow and the external force [see Fig. 2(c)]. The direction of the drift now depends on the sign of the force, but is independent of the boundaries. This is the mechanism proposed in Ref. [6], but it does not explain polymer migration in the presence of a body force alone.

If the external force and pressure gradient drive the polymer in the same direction, the theory predicts that
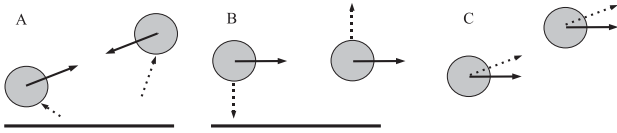
FIG. 2. Illustration of different migration mechanisms. In each figure the solid lines represent the forces while the dashed lines represent the velocities generated by these forces. The velocities can be calculated using Blake's solution [18] for a point source near a planar boundary. (a) The lift due to shear: the tension in the polymer near a solid boundary generates a net velocity away from the boundary. (b) Rotation due to the external field: the velocity field due to the external force on each bead results in a rotation about the center of mass of the polymer. (c) Drift of a rotated polymer: two beads oriented at an angle to the external force drift due to the hydrodynamic interactions between the beads.

the coupled term enhances the migration towards the channel center [Eq. (1)]. The numerical results in Fig. 3 verify this prediction, as seen by comparing the results (Pe = 110) in Fig. 1 with Fig. 3 (Pe$_f$ = 12.5). The relatively weak flow makes only a 10%–20% contribution to the migration. However, polymers of different length have significantly different elution rates; larger polymers migrate more strongly and therefore sample higher velocity streamlines near the center of the channel. Since the migration is primarily driven by the external field, a weak hydrodynamic flow could be used for fractionation, thereby reducing the Taylor dispersion.

In a countercurrent application of the two fields, the polymer tends to orient in different quadrants depending on the relative magnitude of the two driving forces. The polymer now drifts either towards the walls or towards the
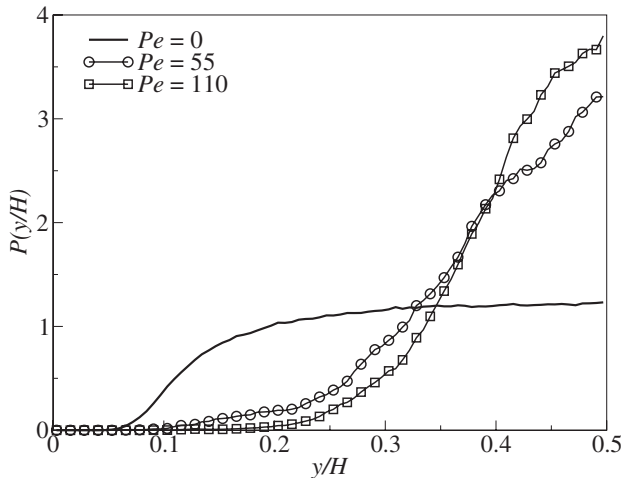
center depending on its mean orientation. The results in Fig. 4 show migration towards the boundaries when the external force is small (Pe < 30), but increasing the force eventually reverses the orientation of the polymer and the polymer again migrates towards the center (Pe > 100). We note as an empirical observation that the peak of the polymer migration towards the wall (Pe = 44) occurs when the polymer is driven with almost equal but opposite velocity by the flow and force.

The numerical results and kinetic theory predictions are in qualitative agreement with a series of experiments measuring the distribution of confined DNA under the combined action of an electric field and a pressure-driven flow [6,7]. These experiments showed a strong migration towards the center in the concurrent application of force and flow, and also the reverse migration towards the boundaries in the countercurrent application. However the experiments do not show a strong migration when the electric field is applied by itself. This suggests that the dominant mechanism in the laboratory experiments [6] is the coupling between the local shear rate and the applied force [Eq. (1)], rather than rotation of the polymer by hydrodynamic interactions with the walls. The channel dimensions in the experiments were about 10 times larger, in comparison with the polymer size, than those in the simulations, which reduces the importance of wall effects. More crucially, the hydrodynamic interactions in polyelectrolyte solutions driven by an electric field are screened by the counterion motion [14]. Screening is neglected in our simulations, which consider only an external body force such as an ultracentrifuge. Nevertheless, if there were no significant hydrodynamic interaction between segments, a polyelectrolyte would just follow the external field without significant transverse motion, even when deformed by a

FIG. 3. Center of mass distributions for concurrent application of an external body force and pressure-driven flow. The solid curve shows the level of migration under the pressure-driven flow only. The flow Peclet number in all three cases is Pe$_f$ = 12.5. The boundary is at $y/H = 0$ and the center of the channel is at $y/H = 0.5$.
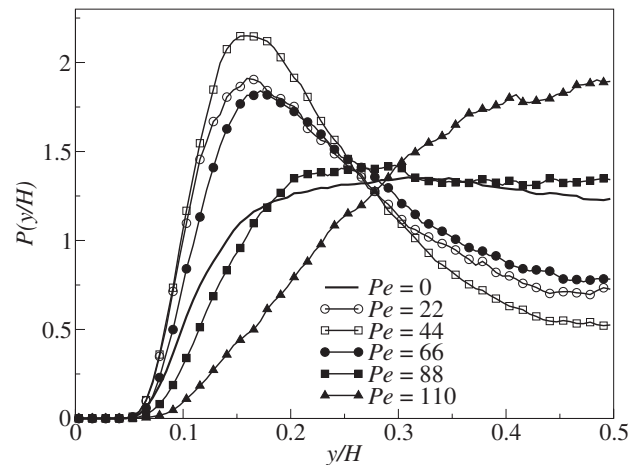
FIG. 4. Center of mass distributions for countercurrent application of an external body force and pressure-driven flow. The solid curve shows the level of migration under the pressure-driven flow only. The flow Peclet number in all cases is Pe$_f$ = 12.5. The boundary is at $y/H = 0$ and the center of the channel is at $y/H = 0.5$.

shear. The rigid-rod model cited in Ref. [7] only shows migration because of hydrodynamic interactions between segments. We have verified this with numerical simulations in which hydrodynamic interactions were excluded. Thus the observation of migration in these experiments [6,7] implies a degree of hydrodynamic interaction on the scale of the polymer.

The fluid velocity field around a polyelectrolyte in an electric field has a dipolar component, decaying as $1/r^3$ [8,15]. We suggest that this dipolar hydrodynamic interaction can account for the observed migration of DNA driven by a combination of electric field and pressure-driven flow [6]. A polyelectrolyte in a weak pressure-driven flow field (Pe $\sim$ 10) is stretched and oriented by the local shear rate in much the same way as a neutral polymer. On average, the polyelectrolyte is then roughly ellipsoidal in shape, with the long axis oriented at 45° to the flow velocity. If an electric field is applied along the same direction as the flow, then the dipolar part of the hydrodynamic interaction causes a weak migration of the polymer in the direction normal to the field. The calculation follows Ref. [8], although they only explicitly considered cases where the electric field was along one of the principal axes of the polymer. Here we show that an order of magnitude estimate of the migration velocity is consistent with the experimental observations.

The equilibrium structure factor, $S(q)$, of a polymer or polyelectrolyte is perturbed by a weak shear flow; the linearized correction is, to within an $\mathcal{O}(1)$ coefficient, $-\mathrm{Pe}_f q_x q_y R_g^2 S(q)$. In an electric field, a polyelectrolyte then has a transverse migration velocity of magnitude $F\mathrm{Pe}_f/\eta\kappa^2 R_g^3$, where F is the total electric force on the polymer, η is the fluid viscosity, and κ is the inverse Debye length. This velocity is small in comparison with the electrophoretic velocity along the channel, $F/\eta L$; the ratio of migration velocity to electrophoretic velocity scales as $\mathrm{Pe}_f L/\kappa^2 R_g^3$. For λ-DNA (48.5 kbp) in 5 mM salt solution, the ratio is of the order of 10^{-2} when $\mathrm{Pe}_f \sim$ 10. This is comparable to experimental measurements ($E = 40$ V/cm) [6], which suggest migration velocities of the order of 10^{-3} cm/sec, in comparison with electrophoretic velocities of the order of 10^{-1} cm/sec. The scaling analysis can be made more quantitative by using kinetic theory to estimate the numerical coefficients.

Additional experiments could be performed to probe the screening length associated with the hydrodynamic interactions in polyelectrolyte solutions. We note that Fig. 3 in Ref. [6] may indicate a weak force-induced migration, although the statistical errors in the data make it inconclusive. A narrower channel would be helpful in promoting hydrodynamic interactions between the polymer and the channel walls, thereby strengthening any force-induced migration. The magnitude of the applied force could be increased by using low-frequency ac fields; since the force-induced migration is quadratic in the field, the direction of migration is independent of the sign. This should make it possible to clearly decide if there is any force-induced migration or not. Screening could also be investigated directly by numerical simulation, either with explicit charges or through a Poisson-Boltzmann approximation [16,17].

In this work, we have shown that confined polymers migrate towards the center of a channel under the application of body forces, due to hydrodynamic interactions between polymer segments and the channel walls. We have developed a kinetic theory that explains these observations at least qualitatively. We note that our observations of polymer migration mirror those of recent experiments with DNA [6,7]. The similarities between the migration of a neutral polymer driven by a body force and a polyelectrolyte driven by an electric field suggest that hydrodynamic interactions in polyelectrolyte solutions are only partially screened [8]. Indeed, if they were fully screened [14] the observed migration would not occur. We have suggested additional laboratory and numerical experiments to further investigate this question.

---

*Electronic address: ladd@che.ufl.edu

[1] L. Fang, H. Hu, and R. G. Larson, J. Rheol. (N.Y.) **49**, 127 (2005).

[2] R. M. Jendrejack, D. C. Schwartz, J. J. de Pablo, and M. D. Graham, J. Chem. Phys. **120**, 2513 (2004).

[3] H. Ma and M. Graham, Phys. Fluids **17**, 083103 (2005).

[4] O. B. Usta, J. E. Butler, and A. J. C. Ladd, Phys. Fluids **18**, 031703 (2006).

[5] J.-L. Viovy, Rev. Mod. Phys. **72**, 813 (2000).

[6] J. Zheng and E. S. Yeung, Anal. Chem. **74**, 4536 (2002).

[7] J. Zheng and E. S. Yeung, Anal. Chem. **75**, 3675 (2003).

[8] D. Long and A. Ajdari, Eur. Phys. J. E **4**, 29 (2001).

[9] O. B. Usta, A. J. C. Ladd, and J. E. Butler, J. Chem. Phys. **122**, 094902 (2005).

[10] P. Ahlrichs and B. Dünweg, J. Chem. Phys. **111**, 8225 (1999).

[11] A. J. C. Ladd, Phys. Rev. Lett. **70**, 1339 (1993).

[12] R. E. Caflisch and J. H. C. Luke, Phys. Fluids **28**, 759 (1985).

[13] T. N. Swaminathan, K. Mukundakrishnan, and H. Hu, J. Fluid Mech. **551**, 357 (2006).

[14] G. S. Manning, J. Phys. Chem. **85**, 1506 (1981).

[15] D. Long, J.-L. Viovy, and A. Ajdari, Phys. Rev. Lett. **76**, 3858 (1996).

[16] J. Horbach and D. Frenkel, Phys. Rev. E **64**, 061507 (2001).

[17] K. Kim, Y. Nakayama, and R. Yamamoto, Phys. Rev. Lett. **96**, 208302 (2006).

[18] J. R. Blake, Proc. Camb. Philos. Soc. **70**, 303 (1971).